INTERNATIONAL JOURNAL OF ADAPTIVE CONTROL AND SIGNAL PROCESSING, VOL. 4, 219–236 (1990)

FREQUENCY-DEPENDENT BURSTING IN ADAPTIVE ECHO CANCELLATION AND ITS PREVENTION USING DOUBLE-TALK DETECTORS

Z. DING AND C. R. JOHNSON JR.
School of Electrical Engineering, Cornell University, Phillips Hall, Ithaca, NY 14853, U.S.A.

AND

W. A. SETHARES
Department of Electrical and Computer Engineering, University of Wisconsin–Madison, Madison, WI 53706, U.S.A.

SUMMARY

Echo cancellation in telephone communications can often be accomplished by using adaptive network echo cancellers. However, under certain circumstances, these generally effective echo cancellers can cause an undesirable bursting phenomenon. In this paper the essential driving force behind bursting is attributed to the correlation between the signal the near-end is to transmit and the signal the near-end receives from the far-end. This correlation and the subsequent potential for temporary destabilization arise as a result of the feedback loop structure of the four-wire telephone circuit. A new test signal which approximately measures this correlation is proposed for use in the double-talk detector scheme that is commonly used to halt adaptation before a mishap such as bursting occurs.

KEY WORDS Bursting Averaging Double-talk detector Adaptive echo cancellation

1. INTRODUCTION

The adaptive network echo canceller has been well established as an effective means of echo removal in telephony networks.[1–4] Like many other adaptive systems, an adaptive echo-cancelling circuit achieves desirable performance when it is adequately excited and when the echo-cancelling circuit is capable of closely modelling the dynamics of the echo path.

A diagram of a typical four-wire telephone circuit is shown in Figure 1, which can be drastically simplified into the model given by Figure 2. At the near-end, the adaptive echo canceller attempts to cancel the echo path transfer function h by its estimate $\hat{h}$. For this adaptive hybrid at the near-end, the desired excitation is the received signal r_{k-n} while the near-end signal v_k acts as a disturbance to the prediction error s_k. The occasional deleterious presence of a large disturbance v_k relative to r_{k-n} (also known as double-talk) is inevitable in any conversation. As a result, the likelihood of success of an adaptive hybrid depends on the degree of decorrelation between the excitation r_{k-n} and the disturbance v_k. If v_k introduces a component into the noisy prediction error s_k that is correlated with r_{k-n}, a 'normal' adaptive algorithm

This paper was recommended for publication by editor T. Durrani

0890–6327/90/030219–18$09.00

Received 1 December 1988
Revised 8 August 1989

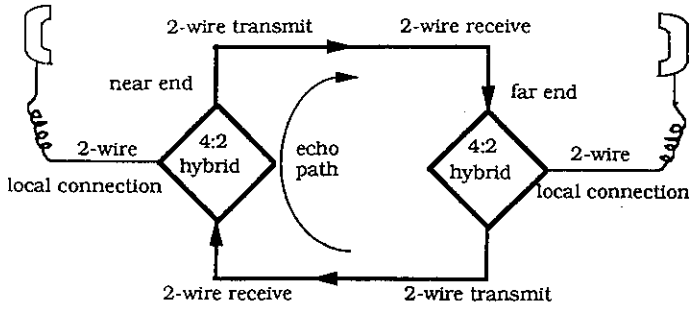

Figure 1. A typical subscriber-loop telephone system

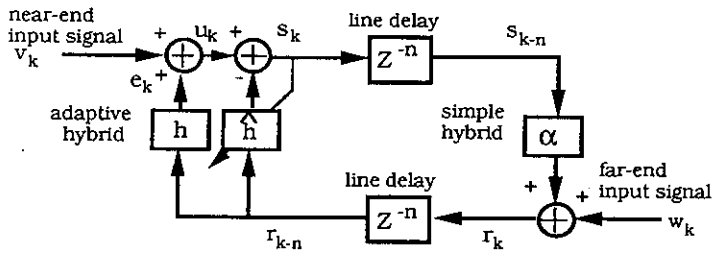

Figure 2. A simplified model for the closed-loop adaptive echo cancellation system

will assume that this component is part of the echo leaking through the hybrid and $\hat{h}$ will be adjusted in an effort to cancel it. This can cause the echo-cancelling system to misbehave by shifting $\hat{h}$ away from h.

The conventional solution to such an ill-conditioned situation is to introduce a 'double-talk detector' (DTD) or 'near-end speech detector' in the adaptive hybrid. The idea is to freeze parameter adaptation when the disturbance v_k is strong compared with the signal r_{k-n}[1-4] so that the adaptation operates only when the disturbance to the prediction error is small. However, if the DTD is designed to be too cautious, it frequently interrupts the adaptation so that the adaptive filter may be unable to sufficiently reduce a substantial parameter error $|h - \hat{h}|$ and hence fail to achieve good echo attenuation much of the time. If the DTD is too bold, the adaptive hybrid may be updated even when the near-end signal v_k is strong enough to misadjust $\hat{h}$. The misadjustment manifests itself as an erroneous value of $\hat{h}$ attempting to keep s_k^2 small. However, in the system model of Figure 2 an excessively large estimation error $|h - \hat{h}|$ and non-zero α can combine to destabilize the feedback circuit formed by the closed telephony loop. In such a situation an undesirable phenomenon called bursting[5] can arise. These bursts are characterized by periods of low-error stable operation interrupted by brief periods of wild oscillation of the received and transmitted signals. Observation of such a phenomenon in real-time benchtop experiments has been reported at Tellabs Research Laboratory, as noted in Reference 5. In fact, it is a phenomenon that is related to bursting in adaptive control[6] and to the self-stabilization behaviour of certain ADPCM schemes which include pole–zero model predictors.[7] The structural property common to all three of these problems is the adaptation of parameters within a feedback loop thereby adjusting the poles of the feedback system. Inappropriate adaptation may lead to a destabilizing parametrization which, if temporary but recurrent, manifests itself as bursting.

The bursting behaviour of an adaptive echo canceller has been previously addressed by Sethares *et al.*[5] The possible temporary instability and subsequent bursting behaviour of the

telephone loop in Figure 2 without a DTD was shown to arise, as expected, due to a large near-end input coupled with a very small far-end input. The analysis of Reference 5 was, however, carried out only for DC and extremely-low-frequency sinusoidal inputs which are nearly DC.

In this paper we study the bursting problem of the configuration of Figure 2 for inputs of sinusoidal signals. This study reveals the frequency dependence of the bursting behaviour, which is anticipated from studies of similarly configured adaptive control systems. Given our improved understanding of this problem, we propose a potentially more effective DTD threshold test involving the correlation rather than the power ratio of appropriate signals.

We begin by formulating the bursting problem of a simple echo cancellation system in Section 2. Assuming sinusoidal inputs, we locate the possible equilibrium points for the average of the parameter estimate dynamics of Figure 2 and show that their location determines the occurrence of bursting (Section 3). By examining conditions under which these equilibria would lead to marginal stability of the telephone loop, we attempt to divide those operating conditions avoiding bursting from those allowing it. Section 3 also delineates the frequency dependence of bursting, with results confirmed by simulations. In Section 4 we propose a new double-talk detector which can act more accurately in halting the algorithm updating. The improved ease in selecting appropriate thresholds for a prespecified parameter error tolerance is also stressed.

2. BASIC ASSUMPTIONS AND PROBLEM FORMULATION OF BURSTING

Our study of echo cancellation in a telephony loop is based on the simple model of Figure 2, for which the following assumptions are made.

(a) Each echo path has only a single scaling parameter—h for the near-end hybrid and α for the far-end hybrid ($h, \alpha \in \mathbb{R}$).
(b) Only the near-end hybrid is adaptive, while the far-end hybrid is not adapted (or is adapted at a much slower rate).
(c) Both the transmission and reception paths introduce delays of n units.

These simplifications are made for the convenience of analysis. Note, however, that similar bursting phenomena can be encountered in the more general settings where h and α represent more complicated transfer functions and when adaptation is present at both ends of the line.[5] The near-end and far-end signals are denoted by v_k and w_k respectively. The received signal at the near-end is denoted by r_{k-n}, the transmitted signal by s_k and the returning echo by e_k, as shown in Figure 2.

To update the parameter $\hat{h}$ of the adaptive echo canceller, the LMS algorithm[8] is implemented, i.e.

$$\hat{h}_k = \hat{h}_{k-1} + \mu s_k r_{k-n} \tag{1}$$

in which μ is the step size and

$$s_k = v_k + (e_k - \hat{e}_k) \tag{2}$$

is the transmitted signal. The echo is given by $e_k = h r_{k-n}$, whose estimate given by the output of the adaptive filter is $\hat{e}_k = \hat{h}_{k-1} r_{k-n}$. The received signal r_{k-n} is formed as

$$r_{k-n} = w_{k-n} + \alpha s_{k-2n} \tag{3}$$

which is just the delayed signal from the far-end hybrid. By denoting the parameter estimate error as $\tilde{h}_k = h - \hat{h}_k$ we can rewrite (1) and (2) as

$$\tilde{h}_k = (1 - \mu r_{k-n}^2)\tilde{h}_{k-1} - \mu r_{k-n} v_k \tag{4}$$

If $(1 - \mu r_{k-n}^2)$ is a contraction and r_{k-n} and v_k are almost uncorrelated such that their product is small on average, then $\tilde{h}_k$ will be expected to converge to a neighbourhood about zero when μ is appropriately chosen. Good echo cancellation is thus achieved. Problems may arise when r_{k-n} is small (i.e. weakening the contraction) but r_{k-n} and v_k are highly correlated such that the (average) forcing term in (4) is large. As a result the echo path may not be well cancelled and misbehaviour such as bursting may occur.

To analyse the bursting phenomenon we shall use the technique of averaging analysis. For the adaptive algorithm of (1) the equilibrium of the averaged system is reached when

$$\text{Avg}\{s_k r_{k-n}\} = 0 \tag{5}$$

By assuming a very small adaptation step size μ, when (5) is satisfied (or for that matter, within a particular time window) the parameter estimate error is effectively invariant, i.e. $\tilde{h}_k \approx \tilde{h}$. As a result the average update in (4) can be written as

$$\begin{aligned}\text{Avg}\{s_k r_{k-n}\} &= \text{Avg}\{v_k r_{k-n}\} + \text{Avg}\{\tilde{h}_{k-1} r_{k-n}^2\} \\ &\approx \text{Avg}\{v_k r_{k-n}\} + \tilde{h}\ \text{Avg}\{r_{k-n}^2\}\end{aligned} \tag{6}$$

where the existence of these averages is implicitly assumed. In such a case the transmitted and received signals are approximated respectively by

$$r_{k+i-n} \approx \frac{1}{1 - \alpha \tilde{h} z^{-2n}} (w_{k+i-n} + \alpha v_{k+i-2n}) \tag{7}$$

$$s_{k+i} \approx \frac{1}{1 - \alpha \tilde{h} z^{-2n}} (v_{k+i} + \tilde{h} w_{k+i-n}) \tag{8}$$

Note that the denominator $1 - \alpha \tilde{h} z^{-2n}$ is zero at $\pm (\alpha \tilde{h})^{1/2n}$ and the closed-loop time-invariant system is stable if and only if $|\alpha \tilde{h}| < 1$.

By setting the average update in (6) to zero in satisfaction of (5) we can obtain the average equilibrium as

$$\tilde{h}^* = -\frac{\text{Avg}\{v_k r_{k-n}\}}{\text{Avg}\{r_{k-n}^2\}} \tag{9}$$

If all the average equilibria $\tilde{h}^*$ are such that $|\alpha \tilde{h}^*| < 1$, then by choosing μ sufficiently small the entire system will be stable and bursting will not occur. If, however, all the closed-loop poles are such that

$$|\alpha \tilde{h}^*| = |\alpha| \frac{|\text{Avg}\{v_k r_{k-n}\}|}{\text{Avg}\{r_{k-n}^2\}} > 1 \tag{10}$$

i.e. outside the stability region $|z| < 1$, then the averaged system is expected to experience problems since it is likely to converge to one of the equilibria $\tilde{h}^*$. that destabilize the closed-loop system.

The potential for bursting results from a large near-end signal v_k that dominates the prediction error e_k in s_k of (2). When the disturbance v_k is correlated with the excitation signal r_{k-n}, the LMS algorithm reacts as if it is part of the echo and, in an effort to cancel the disturbance, $\tilde{h}_k$ is misadjusted, which causes a possibly large error $\tilde{h}_k$. Suppose v_k and w_k are independent and both are zero-mean, then $\text{Avg}\{v_i w_j\} \approx 0$. Hence, when the disturbance v_k dominates e_k (such that $v_k + e_k \approx v_k$),

$$\begin{aligned}\text{Avg}\{r_{k-n} v_k\} &= \text{avg}\{[w_{k-n} + \alpha(e_{k-2n} + v_{k-2n})] v_k\} \\ &\approx \alpha\ \text{Avg}\{(e_{k-2n} + v_{k-2n}) v_k\} \approx \alpha\ \text{Avg}\{v_k v_{k-2n}\} \approx \alpha R_v(2n)\end{aligned} \tag{11}$$

where R_v is defined as the correlation function of v_k. From (4) and (11) it can be concluded that a highly correlated near-end signal v_k results in a larger forcing in (4) and hence is more likely to cause a large parameter error $\tilde{h}$ (perhaps bursting when (10) holds) by the adaptive system.

Consequently, we would like the autocorrelation $R_v(2n)$ to be small in order to avoid bursting and to reduce the parameter estimation error $\tilde{h}$. This correlation can be greatly reduced if v_k is a wide-band signal and/or if the transmission delay n is very long. The rare occurrence of bursting in very-long-distance telephone communications corroborates this observation. If α is also an adaptive hybrid, then its stable performance will in turn require w_k to have a wide-band spectrum as well. It is clear from (10) and (11) that good echo cancellation at the far-end hybrid (i.e. $\alpha \approx 0$) can improve the performance at the near-end. Hence bursting should be extremely rare if both hybrids have settings that offer significant echo cancellation and if both inputs are wide-band signals.

Through the above analysis it is evident that misperformance should be expected of the near-end adaptive echo canceller if a strong, narrow-band signal is present at the near-end while the far-end signal is relatively weak. In the next section we analyse the occurrence of bursting when both inputs are sinusoids (signals with the narrowest bandwidth), and in Section 4 we discuss a common measure to prevent the misbehaviour of adaptive algorithms given such an ill-conditioned circumstance; namely, the application of a double-talk detector.

3. BURSTING ANALYSIS UNDER SINUSOIDAL INPUTS

3.1. Averaging analysis of bursting

To understand how bursting occurs, consider the situation when the input signals v_k and w_k are sinusoidal signals of different frequencies, i.e.

$$v_k = A_1 \cos(\omega_1 k) \tag{12}$$

$$w_k = A_2 \cos(\omega_2 k + \psi) \tag{13}$$

where both frequencies $\omega_1 \neq \omega_2$ are normalized with respect to the sampling frequency so that $0 < \omega_1, \omega_2 < \pi$. For analytical simplicity, also assume that ω_1/ω_2 is rational.

As noted with (5), the adaptive algorithm of (12) achieves its average equilibrium[8] when

$$\text{Avg}\{s_k r_{k-n}\} = \frac{1}{N} \sum_{i=1}^{N} s_{k+i} r_{k+i-n} = 0 \tag{14}$$

where $N \in \mathbb{Z}_+$ is the least common multiple of $2\pi/\omega_1$ and $2\pi/\omega_2$. $\text{Avg}\{v_i w_j\}$ is approximately zero for $\omega_1 \neq \omega_2$ and thus from (7) and (8)

$$\begin{aligned}\text{Avg}\{s_k r_{k-n}\} &\approx \frac{\alpha}{N} \sum_{i=1}^{N} \frac{A_1^2 \cos[\omega_1(k+i-2n)+\phi_1]\cos[\omega_1(k+i)+\phi_1]}{|1-\alpha\tilde{h}e^{-j2n\omega_1}|^2} \\ &\quad + \frac{\tilde{h}_k}{N} \sum_{i=1}^{N} \frac{A_2^2 \cos^2[\omega_2(k+i-n)+\phi_2]}{|1-\alpha\tilde{h}^{-j2n\omega_2}|^2} \\ &\approx \frac{\alpha}{2} \frac{A_1^2 \cos(2n\omega_1)}{|1-\alpha\tilde{h}e^{-j2n\omega_1}|^2} + \frac{\tilde{h}}{2} \frac{A_2^2}{|1-\alpha\tilde{h}e^{-j2n\omega_2}|^2}\end{aligned} \tag{15}$$

in which $\phi_1 = \angle(1-\alpha\tilde{h}e^{-j2n\omega_1})^{-1}$ and $\phi_2 = \psi + \angle(1-\alpha\tilde{h}e^{-j2n\omega_2})^{-1}$. Therefore in this case the

solution $\tilde{h} = \tilde{h}^*$ to (14) is

$$\alpha\tilde{h}^* = -\frac{|1 - \alpha\tilde{h}^* e^{-j2n\omega_2}|^2}{|1 - \alpha\tilde{h}^* e^{-j2n\omega_1}|^2} \cos(2n\omega_1)\left(\frac{\alpha A_1}{A_2}\right)^2 \tag{16}$$

Hence we have $\tilde{h}^* \in \mathbb{R}$ and

$$\operatorname{sgn}(\alpha\tilde{h}^*) = -\operatorname{sgn}[\cos(2n\omega_1)] \tag{17}$$

It should be noted that (16) is a cubic equation for which there can be one or three real solutions. From the above analysis we can get the following.

Proposition 1

If an $\tilde{h}^*$ given by (16) is such that $|\alpha\tilde{h}^*| < 1$, then it is unique within $\alpha\tilde{h}^* \in (-1, 1)$. In addition, it is a locally stable equilibrium of the averaged system. If the step size is very small and $|\alpha\tilde{h}_k| < 1$, then $\tilde{h}_k$, starting within $\alpha\tilde{h}_k \in (-1, 1)$, will converge to and remain in the neighbourhood of $\tilde{h}^*$.

Proof. See Appendix.

If, however, (16) only holds when $|\alpha\tilde{h}^*| > 1$, then no stable equlibria exist for the averaged system and we anticipate bursting. In this case there is a tendency for the slowly time-varying poles $\pm(\alpha\tilde{h}_k)^{1/2n}$ to move across the stability boundary $|\alpha\tilde{h}_k| = 1$. As a result the signal r_k will quickly grow (at least temporarily) and bursting occurs. When r_k becomes so large that the factor $1 - \mu r_{k-1}^2$ is small enough to be dominant in (6), $\tilde{h}_k$ begins to shrink. Once $|\alpha\tilde{h}_k|$ drops below unity, r_k shrinks until $\tilde{h}_k$ again begins to rise and cross the stability boundary, and so on. This characterizes the process of bursting, much as in Reference 5. Consequently, we have the following.

Proposition 2

If all the solutions $\tilde{h}^*$ of (16) are such that $|\alpha\tilde{h}^*| > 1$, and if $\alpha\tilde{h}_k$ is initialized such that $|\alpha\tilde{h}_k| < 1$, then on the average $\alpha\tilde{h}_k$ will either be driven across the stability boundary or move arbitrarily close to it.

Proof. See Appendix.

Remarks

(i) If the average $\alpha\tilde{h}_k$ moves across the stability boundary $|\alpha\tilde{h}_k| = 1$, then bursting will occur.

(ii) If the average $\alpha\tilde{h}_k$ moves arbitrarily close to the stability boundary such that $1 - \varepsilon < |\alpha\tilde{h}_k| < 1$, then the averaged system is marginally stable. Owing to the intrinsic deviations from its average by the actual algorithm, $\alpha\tilde{h}_k$ will at least temporarily cross the stability boundary, which should also cause bursting.

In summarizing Proposition 2 and the remarks following it, bursting is anticipated if all the solutions $\tilde{h}^*$ of (16) are outside the stability boundary $|\alpha\tilde{h}^*| = 1$.

It is now evident that under narrow-band inputs, $|\alpha\tilde{h}^*| > 1$ indeed delineates the occurrence of bursting. We now proceed to discuss the dependence of this condition on the input signal characteristics.

3.2. *Sufficient condition to avoid bursting*

From the analysis of Section 3.1, the equilibria of the average echo cancellation system are characterized by the stable solution (i.e. $|\alpha\tilde{h}^*| < 1$) of

$$\alpha\tilde{h}^* = -\frac{1 + (\alpha\tilde{h}^*)^2 - 2\alpha\tilde{h}^* \cos(2n\omega_2)}{1 + (\alpha\tilde{h}^*)^2 - 2\alpha\tilde{h}^* \cos(2n\omega_1)} \cos(2n\omega_1)M \tag{18}$$

where $M = (\alpha A_1/A_2)^2$ for sinusoidal inputs. Clearly the magnitude of $\alpha\tilde{h}^*$ and hence the occurrence of bursting depend upon the magnitudes of the input signals w_k and v_k. The following simple result is important.

Proposition 3

For $\alpha\tilde{h}^*$ that satisfies (16), the inequality

$$\left| \frac{|1 - \alpha\tilde{h}^* e^{-j2\omega_2}|^2}{|1 - \alpha\tilde{h}^* e^{-j2\omega_1}|^2} \cos(2\omega_1) \right| \leqslant 1 \tag{19}$$

holds for all $\omega_1, \omega_2 \in \mathbb{R}$.

Proof. See Appendix.

Thus we arrive at a sufficient condition to avoid bursting.

Corollary

For the adaptive echo cancellation system (1)–(4) with two sinusoidal inputs of different frequencies ω_1, ω_2 and amplitudes A_1, A_2, suppose $(\alpha A_1/A_2)^2 < 1$. Then it follows from (18) and (19) that

$$|\alpha\tilde{h}^*| \leqslant \left(\frac{\alpha A_1}{A_2}\right)^2 < 1 \tag{20}$$

Hence the average equilibria are stable and bursting can be avoided.

Look at Figure 2 carefully. The corollary indicates that if the near-end signal is small enough so that its power after passing through the far-end echo path, $(\alpha A_1)^2/2$, is smaller than the signal power of the far-end input, $A_2^2/2$, then the overall adaptive system will remain stable and bursting can be avoided. This agrees with the character of the result given in Reference 5 that strong near-end inputs coupled with very weak far-end signals can cause bursting. This observation also corroborates the use of the power ratio test in the common DTD.

3.3. *The frequency dependence of bursting*

In Section 3.2 it has been shown that when the input signals are sinusoids and $M < 1$, then $|\alpha\tilde{h}^*| < 1$ and bursting can be avoided. In any case the resulting values of average equilibrium $\alpha\tilde{h}^*$ clearly depend on the frequencies ω_1, ω_2 of the input signals. To illustrate the frequency dependence of the bursting behaviour we shall again assume sinusoidal inputs and discuss the situation when the amplitude condition $M < 1$ is violated.

Proposition 4

If $M > 1$, then (ω_1, ω_2) pairs exist such that some solutions of (18) satisfy $|\alpha\tilde{h}^*| > 1$ and other (ω_1, ω_2) pairs exist such that some solutions of (18) satisfy $|\alpha\tilde{h}^*| < 1$.

Proof. See Appendix.

This indicates that the occurrence of bursting for this system is input-frequency-dependent. Given $M \geqslant 1$, the pair (ω_1, ω_2) determines the solutions $\alpha\tilde{h}^*$ to (18) and therefore the occurrence of bursting. Consider the case when the transmission delay is $n = 1$ and when only one real solution $\alpha\tilde{h}^*$ exists for (18) (e.g. $M \leqslant 8$). Then, on the basis of equation (18), we can plot the contour of $\{(\omega_1, \omega_2): |\alpha\tilde{h}^*| = 1\}$ on the ω_1–ω_2 plane, which separates the set $\{(\omega_1, \omega_2): |\alpha\tilde{h}^*| < 1\}$ for which a locally stable equilibrium exists and the set $\{(\omega_1, \omega_2): |\alpha\tilde{h}^*| > 1\}$ for which bursting tends to occur. This procedure separates 'bursting' from 'non-bursting' frequency pairs. The results for $M = 2, 5$ and 8 are given in Figures 3(a)–3(c), respectively. The shaded areas, which are labelled 'bursting regions' in these figures, represent the set $\{(\omega_1, \omega_2): |\alpha\tilde{h}^*| > 1\}$ in which bursting occurs. The likelihood of bursting increases with an increase in M, since if we have a bigger M, more pairs of (ω_1, ω_2) fall in the bursting region.

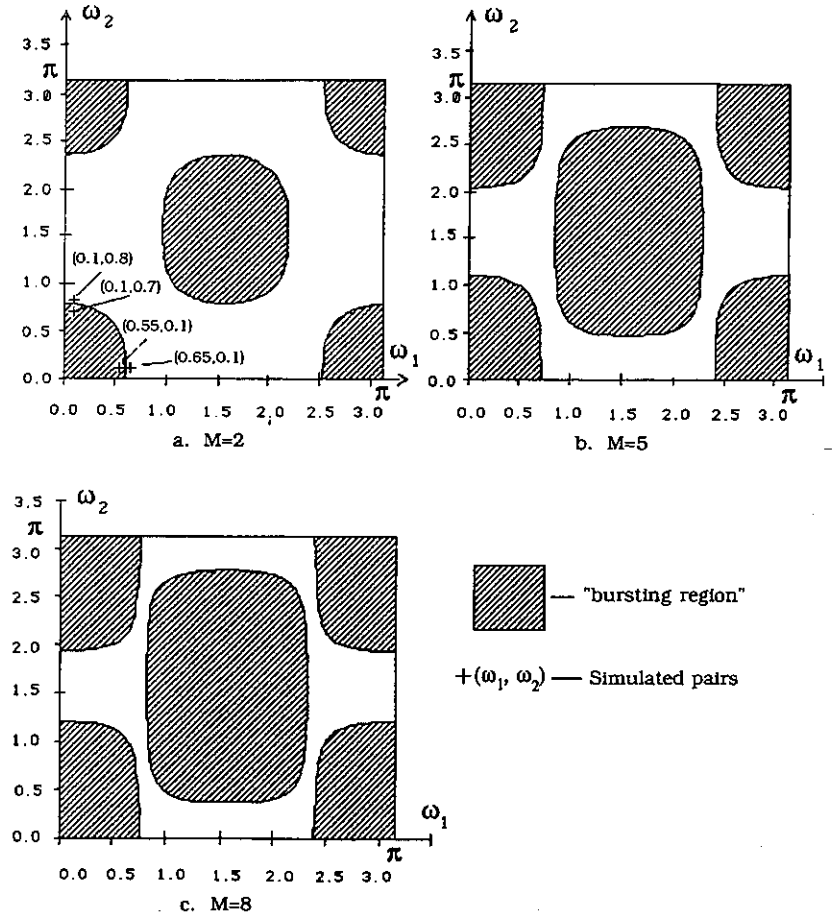

Figure 3. 'Bursting regions' of the adaptive echo canceller for $M = 2$, 5 and 8 when the transmission line delay is $n = 1$

When M drops to unity, each separate shaded area contracts to merely one dot at its centre:

$$\{(\omega_1, \omega_2),\ \cos(2\omega_1) = \cos(2\omega_2) = \pm 1\} \tag{21}$$

If M is less than unity, all the shaded areas simply disappear. On the other hand, if M becomes excessively large, then the shaded area will cover almost the entire ω_1–ω_2 plane, except at lines where $\cos(2\omega_1) = 0$. These properties graphically summarize the analysis of the preceding sections.

From Figure 3 one can see that bursting is more likely to occur at points where $|\cos(2\omega_1)| \approx 1$ and at the same time $\cos(2\omega_1) \approx \cos(2\omega_2)$. The reason is that at these points

$$\left| \left| \frac{1 + (\alpha\tilde{h}^*)^2 - 2\alpha\tilde{h}^* \cos(2\omega_2)}{1 + (\alpha\tilde{h}^*)^2 - 2\alpha\tilde{h}^* \cos(2\omega_1)} \right| \cos(2\omega_1) \right| \approx |\cos(2\omega_1| \approx 1 \tag{22}$$

and if $M > 1$, $|\alpha\tilde{h}^*|$ is more likely to be greater than unity and bursting is more likely to occur.

Simulation studies confirmed the above behaviour of the system. Figure 3(a) indicates different (ω_1, ω_2) pairs for which simulations were made when both inputs were purely sinusoidal waves. A step size of $\mu = 0{\cdot}05$ and zero-parameter estimate $\hat{h}(0) = 0$ were used and the true echo path parameters were set as $\alpha = h = 0{\cdot}1$ in all simulations. For $M = 1$, bursting did not occur even after tens of thousands of iterations with frequency pairs $(\omega_1, \omega_2) = (0{\cdot}1, 0{\cdot}7)$ and $(0{\cdot}55, 0{\cdot}1)$. However, when $M = 2$, which puts the previous two pairs barely inside the shaded region, bursting occurs within a few thousand iterations as shown in Figures 4(a) and 4(b). We also simulated frequency pairs $(\omega_1, \omega_2) = (0{\cdot}1, 0{\cdot}8)$ and $(0{\cdot}65, 0{\cdot}1)$ under the condition $M = 2$. Since they are both slightly outside the shaded areas, no bursting was expected to occur and our simulation results confirmed this. But for $M = 5$, both pairs are inside the bursting area, and bursting occurred in our simulations as illustrated in Figures 5(a) and 5(b). Note that, as in the examples, the bursting need not represent a catastrophic loss in system performance but does represent a degradation of performance. Also note that in the lengthy simulations of Figures 4(a), 4(b) and 5(b), only one of every 50 simulated samples was plotted when the system was not close to bursting, and every sample was displayed when bursting occurred. Therefore the increased darkness of r_k in the neighbourhood of bursting does not necessarily represent an intensified oscillation by the signal r_k.

An important effect is the length of the delays between the near-end and far-end. For

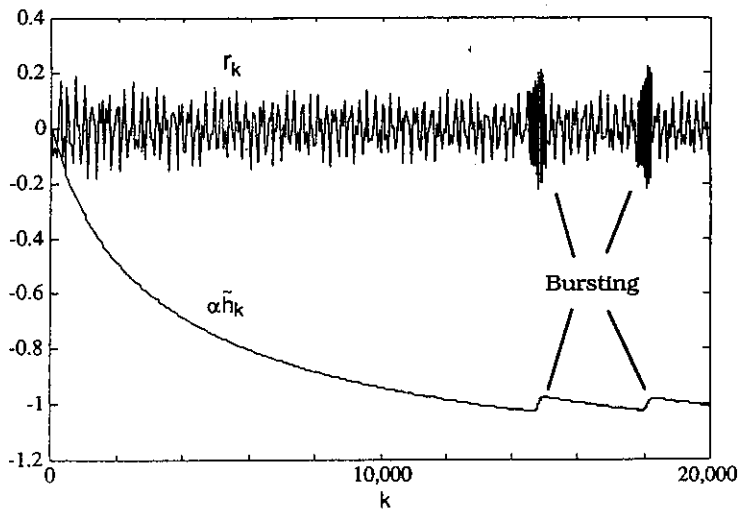

Figure 4(a). Simulation with frequency pair $(0{\cdot}1, 0{\cdot}7)$ shows bursting within 18 000 iterations for $M = 2$

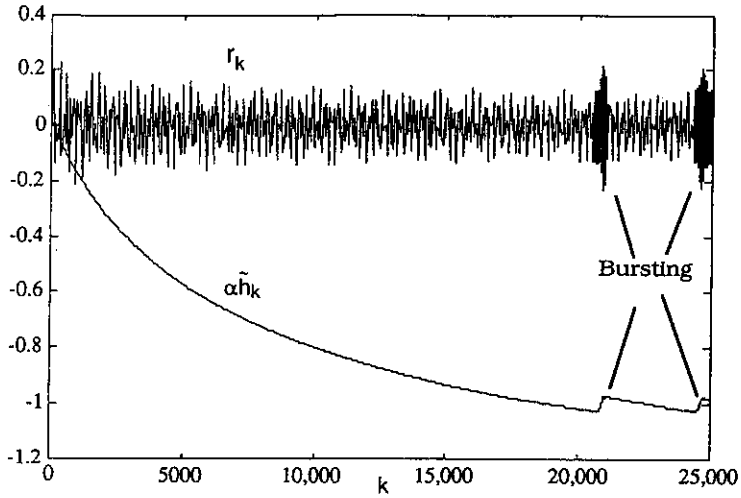

Figure 4(b). Simulation with frequency pair (0·55, 0·1) shows bursting within 22 000 iterations for $M = 2$

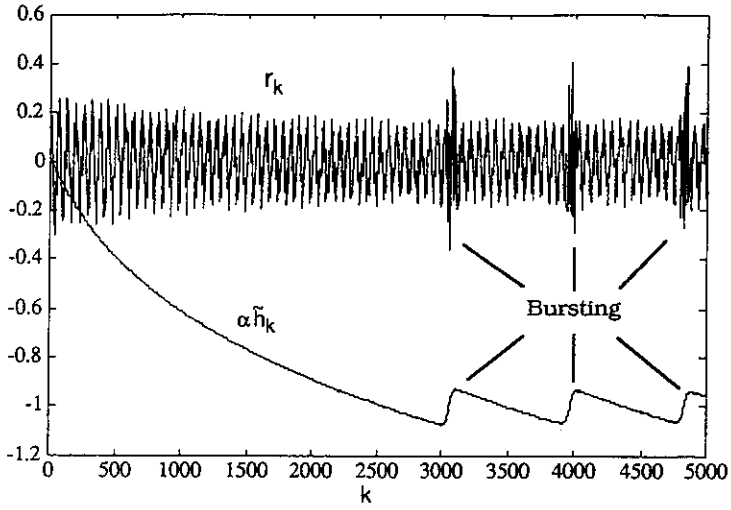

Figure 5(a). Simulation with frequency pair (0·1, 0·8) shows bursting within 4000 iterations for $M = 5$ (one of every five samples is plotted)

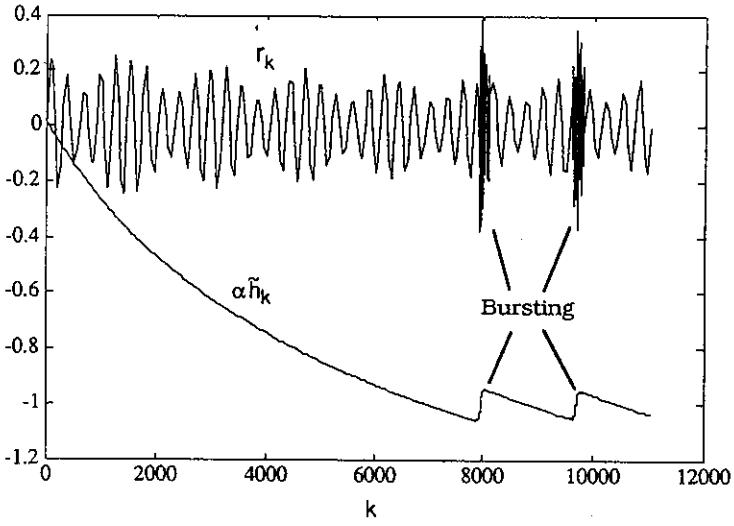

Figure 5(b). Simulation with frequency pair (0·65, 0·1) shows bursting within 10 000 iterations for $M = 5$

connections where a delay of n samples is present in each path, (18) means that bursting is more likely to occur near $|\cos(2n\omega_1)| \approx 1$ and $\cos(2n\omega_1) \approx \cos(2n\omega_2)$. In fact, a plot similar to Figure 3 will show arrays of smaller areas of bursting centred around points

$$\{(\omega_1, \omega_2),\ \cos(2n\omega_1) = \cos(2n\omega_2) = \pm 1\} \tag{23}$$

This suggests that in transmitting narrow-band signals over a telephone system with adaptive echo cancellers, one should avoid using similar carriers (modulo π/n) for the two input signals. When bursting does not occur owing to insufficient signal amplitude disparity, using different carrier frequencies can reduce the parameter estimation error $\tilde{h}$. This practice is known in digital communication systems as offset clock frequency transmission.

4. A NEW DOUBLE-TALK DETECTOR

As noted earlier, double-talk detectors (DTDs) are commonly used to prevent inappropriate adaptation that can cause excessively large parameter estimation error and possibly bursting due to the presence of a strong near-end signal in an adaptive echo cancellation system. A DTD turns off the adaptation by setting $\mu = 0$ if a test signal, ideally an indicator of when the algorithm adaptation is seriously impaired by the near-end input, exceeds a predetermined threshold T.

Two factors are crucial to the effectiveness of DTDs, namely the selection of the test signal and the determination of the threshold. The test signal should truly reflect the seriousness of impairment caused by the near-end input on the adaptive algorithm. An inappropriately chosen test signal can caused the DTD either to be too cautious and turn off the adaptation when the influence of the near-end signal is actually not so damaging, or to be too bold and continue the adaptation even when the near-end signal may result in a large parameter estimation error and possibly bursting. Similarly, an unwisely selected threshold T can be so low as to stop the adaptation too frequently, in which case the echo canceller may not be able to adequately track the time-varying characteristics of the echo path. This threshold can also be too high to stop the adaptation before the parameter estimation error becomes undesirably large.

The conventional DTD merely tests the ratio of averaged (over some time window) powers between the received signal r_{k-n} and the signal $u_k = v_k + hr_{k-n}$, which is approximately v_k when v_k is large and the echo leaking through the near-end hybrid is reasonably small. From (9)–(11) it is clear that this test signal does not determine the magnitude of the average prediction error $\tilde{h}$ and hence is not truly indicative of the necessity to halt the adaptation. For example, the near-end signal may have substantial power but very wide bandwidth. Though it results in a huge conventional test signal and stops the adaptation, its true influence on the convergent parametrization of the averaged system might be insignificant because of its extremely small autocorrelation $R(2n)$. Moreover, the choice of this threshold usually has to be made through trial and error, which is a major weakness of the conventional DTD. We shall propose, through the following discussion, a new DTD which provides a test signal with an easier-to-select threshold.

4.1. *A new double-talk detector*

The analysis in Section 2 suggests the use of a test signal different from the conventional one. Instead of the ratio of average powers, the test signal should be given by

$$T_1 = \frac{|\operatorname{Avg}\{v_k r_{k-n}\}|}{\operatorname{Avg}\{r_{k-n}^2\}} \tag{24}$$

Since this ratio is the key factor in determinng the magnitude of the equilibrium for the averaged system, it can indicate more accurately the impairing influence of the near-end input on the algorithm. To avoid bursting, the test signal can be compared against the threshold $\Theta = (1-\delta)/|\alpha_{\max}|$ ($\delta < 1$) and the algorithm frozen when $T_1 \geqslant \Theta$. As a result, given relatively smooth behaviour due to a small step size μ, halting the adaptation when $T_1 \geqslant \Theta$ will result in the 'convergent' average $\tilde{h}$, i.e. $\tilde{h}^*$, satisfying

$$|\alpha\tilde{h}^*| = |\alpha| \frac{|\text{Average}\{v_k r_{k-n}\}|}{\text{Average}\{r_{k-n}^2\}} \leqslant 1-\delta \tag{25}$$

according to (24), and bursting can then be prevented.

Generally one would like to choose the threshold Θ ($\geqslant 0$) large enough to achieve rapid convergence and good tracking ability but also small enough to maintain tolerable parameter estimation error. Note that the performance of the near-end echo canceller as measured by the signal-to-noise (echo) ratio (SNR) of its transmitted signal s_k is directly related to the parameter error $\tilde{h}$ through

$$\text{SNR} = \frac{\text{E}\{v_k^2\}}{\text{E}\{(s_k - v_k)^2\}} = \frac{\text{E}\{v_k^2\}}{\text{E}\{(\tilde{h}r_{k-1})^2\}} = \frac{\text{E}\{v_k^2\}}{\tilde{h}^2\text{E}\{(r_{k-1})^2\}} \tag{26}$$

Therefore the asymptotic performance of the echo canceller is better if the convergent prameter error $|\tilde{h}|$ is smaller. Large $|\tilde{h}|$ degrades performance even though $|\alpha\tilde{h}|$ may not be large enough to cause bursting. The new test signal T_1 has the advantage that an appropriate threshold Θ can be easily determined from the allowable parameter estimation error $|\tilde{h}|$. For instance, given a constant $\varepsilon > 0$, turning off the algorithm when

$$T_1 \geqslant \Theta = \varepsilon \tag{27}$$

would result in $|\alpha\tilde{h}^*| \leqslant |\alpha\varepsilon|$ and consequently $|\tilde{h}^*| \leqslant \varepsilon$. This would keep the average prediction error $|\tilde{h}^*|$ less than or equal to ε when adequately initialized, and the real-time eror $\tilde{h}_k$ should be at most in the neighbourhood of ε.

Unfortunately, the signal v_k needed to construct T_1 is not accessible at the near-end hybrid. Thus an approximation has to be used to form the test signal. As with the conventional test signal justification, when the echo path parameter h is small (i.e. $h \ll 1$), the signal u_k is a good estimate of v_k when v_k is substantial. Therefore the actual test signal we propose is

$$T_n = \frac{|\text{Average}\{u_k r_{k-n}\}|}{\text{Average}\{r_{k-n}^2\}} \left(= \left| \frac{\text{Average}\{v_k r_{k-1}\}}{\text{Average}\{r_{k-n}^2\}} + h \right| \right) \tag{28}$$

Consequently a threshold of value $\Theta \geqslant 0$ can only guarantee that

$$|\tilde{h}^*| \leqslant \Theta + |h| \tag{29}$$

Thus, in order to keep the parameter estimate at most in the ε-neighbourhood of h, our DTD is to halt the adaptation algorithm when the test signal T_n exceeds a threshold $\Theta \leqslant \varepsilon$.

It should be noted that using s_k in place of u_k in T_n as a better estimate of v_k is inadvisable since the adaptive system is to reduce the correlation between s_k and r_{k-n} no matter how big $|\alpha\tilde{h}|$ might be. Thus the adaptive system using such a DTD risks the possibility of extremely poor performance and even bursting. Simulations have confirmed the possible occurrence of such misbehaviour.

As noted earlier, the conventional DTD halts the adaptation whenever the test signal

$$T_c = \frac{\text{Average}\{u_{k+i}^2\}}{\text{Average}\{r_{k+i-1}^2\}} \tag{30}$$

exceeds a threshold Θ. But for this test signal, the relationship between T_c and the acceptable parameter error ε is not simple. It is very hard to determine a threshold T_c so that $|\tilde{h}|$ is at most in the neighbourhood of ε for all possible input signals. Differences in signal power, carrier frequency and bandwidth will affect the average parameter error $\tilde{h}$. The difficult task of optimizing the threshold Θ over the set of all possible inputs is usually accomplished through trial and error in practice.

4.2. *A simple example*

The following example is given to illustrate the difficulty in determining an appropriate threshold for the conventional DTD and the potential advantage of using the newly proposed DTD. For sinusoidal input signals given by (12) and (13), take $\omega_1 = 0{\cdot}3$, $\omega_2 = 0{\cdot}1$, $n = 1$, $A_2 = 0{\cdot}1$ and $\psi = 1$ rad. Assume that $\alpha = h = 0{\cdot}1$. Given these conditions, both test signals T_n and T_c can be calculated. Figure 6(a) illustrates the conventional T_c for $A_1 = 0{\cdot}1, 0{\cdot}2, \ldots, 1{\cdot}0$ as a function of a (fixed) prediction error $\tilde{h}$. For each A_1 the average equilbrium $\tilde{h}^*$ can be obtained through (16); these are connected to form a dashed curve in Figure 6(a). Similarly, Figure 6(b) displays the new T_n for the same values of A_1 and superimposes the average equilibria curve for various A_1.

From Figures 6(a) and 6(b) one can predict the average behaviour of $\tilde{h}_k$ of the adaptive system given the specific sinusoidal input signals. Without a DTD, on average $\tilde{h}_k$ will move until (16) is satisfied. In terms of Figure 6(a) or 6(b), $(\tilde{h}, T_c)$ or $(\tilde{h}, T_n)$ will move 'along' a solid line corresponding to the particular A_1 towards the point where this line interesects the dashed line of average equilibria $\tilde{h}^*$. When a DTD is used, $\tilde{h}_k$ will move in exactly the same way as long as the test signal is below the preset threshold; $\tilde{h}_k$ stops moving shortly after the test signal grows above the threshold or when the initialization causes the test signal to start above the threshold.

Using Figures 6(a) and 6(b) we can decide the thresholds needed in each case to achieve $|\tilde{h}| \leqslant \varepsilon$. Usually the threshold is chosen as large as possible to maintain good tracking ability. Suppose, for this example, that we wish to have $|\tilde{h}| \leqslant 1$. Then Figure 6(a) indicates that $\Theta_c = 10$ seems to be the threshold we should choose for the conventional DTD in order to keep

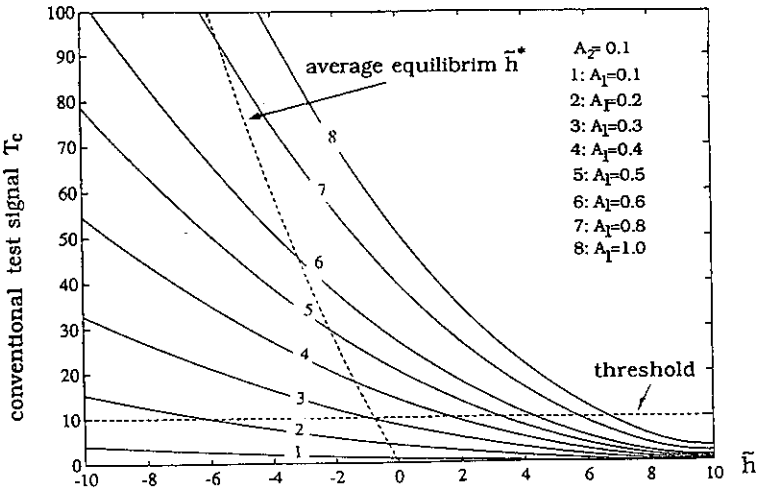

Figure 6(a). Precalculated T_c and average equilibria of the system for different values of near-end A_1 when $\omega_1 = 0{\cdot}3$, $\omega_2 = 0{\cdot}1$

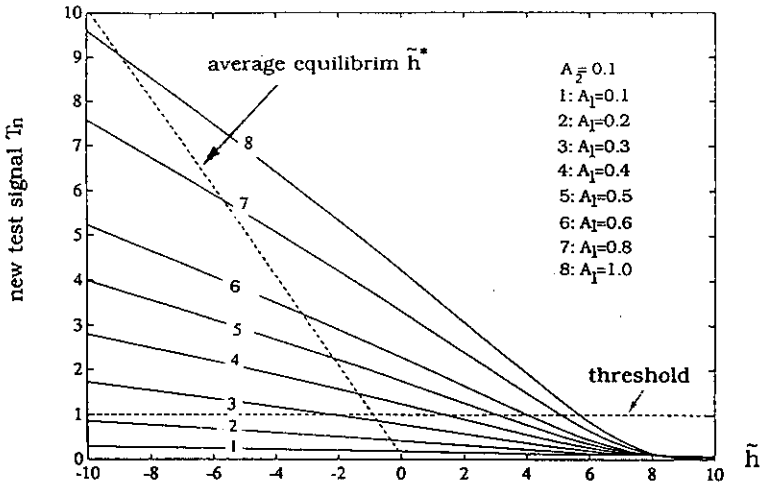

Figure 6(b). Precalculated T_n and average equilibria of the system for different values of near-end A_1 when $\omega_1 = 0{\cdot}3$, $\omega_2 = 0{\cdot}1$

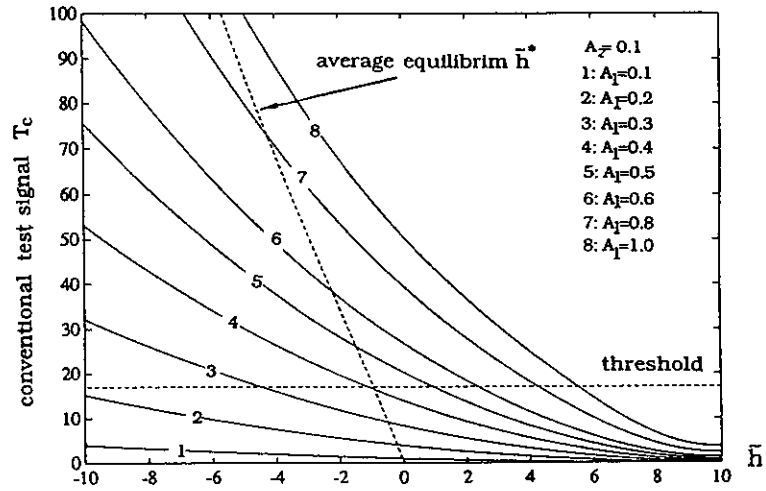

Figure 6(c). Precalculated T_c and average equilibria of the system for different values of near-end A_1 when $\omega_1 = 0{\cdot}5$, $\omega_2 = 0{\cdot}1$

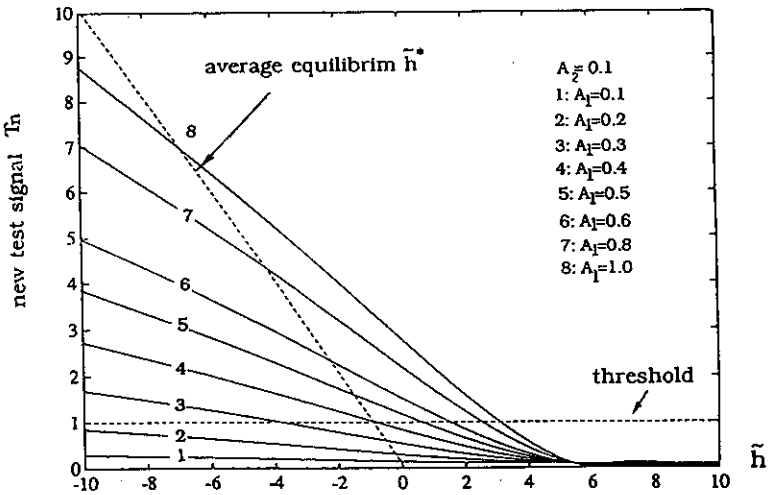

Figure 6(d). Precalculated T_n and average equilibria of the system for different values of near-end A_1 when $\omega_1 = 0{\cdot}5$, $\omega_2 = 0{\cdot}1$

$|\tilde{h}^*| \leqslant 1$ whatever A_1 is present. Figure 6(b) shows that $\Theta_n = 1$ should be the threshold to choose for the new DTD. In both cases the threshold is chosen as the value of the test signal corresponding to $|\tilde{h}^*| \leqslant 1$.

Notice that in practice the frequencies of the input signals are unknown and $\Theta_c = 10$ may not be a wise choice for other frequencies. For example, if we have $\omega_1 = 0{\cdot}5$ and $\omega_2 = 0{\cdot}1$ instead, then redrawing Figure 6(a) for this pair of frequencies as in Figure 6(c) shows that the preferred threshold now becomes $\Theta_c = 17$. Therefore, without the knowledge of the actual input signals, a compromise threshold for the conventional DTD may have to be chosen after numerous trials. On the other hand, the same value of the threshold for the new DTD, i.e. $\Theta_n = 1$, can be chosen without the help of Figure 6(b) merely by following the proposed guideline that Θ_n be slightly smaller than $\varepsilon = 1$. Even if the signal frequencies are now $\omega_1 = 0{\cdot}5$ and $\omega_2 = 0{\cdot}1$, the redrawing of Figure 6(b) as in Figure 6(d) shows that $\Theta_n = 1$ is still the preferred choice of the threshold for the new DTD. This seems to give the new DTD an advantage in practical applications when the input signal frequencies are unknown and figures such as Figure 6(a) are in fact unavailable.

It can be inferred from Figures 6(a) and 6(b) that the conventional DTD is more sensitive to the value of parameter estimation initialization in comparison with the new DTD. Suppose that to achieve $|\tilde{h}| \leqslant 1$, $\Theta_c = 10$ and $\Theta_n = 1$ are chosen for the two DTDs. For $0{\cdot}1 \leqslant A_1 \leqslant 0{\cdot}2$ the $\tilde{h}^*$ are very small as shown in Figures 6(a) and 6(b); thus the parameter error will converge to $|\tilde{h}| \leqslant 1$ when no DTD is used. When the conventional DTD is used, the adaptation will be stopped once T_c exceeds $\Theta_c = 10$. Thus, even though $0{\cdot}1 \leqslant A_1 \leqslant 0{\cdot}2$, if the algorithm is initialized such that $\tilde{h}_0 < -6{\cdot}5$, the test signal will be above the threshold and the algorithm will be halted almost instantaneously so that $\tilde{h} \approx \tilde{h}_0 < -6{\cdot}5$ will be maintained. However, if the new DTD is used, the test signal will be below $\Theta_n = 1$ for $0{\cdot}1 \leqslant A_1 \leqslant 0{\cdot}2$ even when $|\tilde{h}_0| = 10$. Therefore the algorithm will not be halted for $|\tilde{h}_0| \leqslant 10$ and the parameter error will converge to the desirable $|\tilde{h}| \leqslant 1$. Our simulations illustrated this sensitivity.

This example demonstrates an essential difference between these two DTDs. It shows that both DTDs can help to prevent the occurrence of excessively large parameter error if the respective threshold is appropriately chosen and if the parameter estimate is adequately initialized. The appropriate threshold for the conventional DTD has to be chosen experimentally, while the guidelines to determine an appropriate threshold for the new DTD are more helpful, which seems to be an important advantage for using the new DTD. Furthermore, the new DTD proposed here more accurately indicates the need to halt the adaptation and hence exhibits less sensitivity to the initialization of the parameter estimate in comparison with the conventional DTD.

5. CONCLUSIONS

We have studied the bursting behaviour of a simple adaptive echo canceller under sinusoidal signal inputs and uncovered its frequency dependence. We have derived not only an input magnitude condition but also an input frequency condition for burstng avoidance. These results may lead to a better understanding of the excitation requirements of an adaptive echo canceller in a feedback environment. We have reaffirmed the importance of the decorrelation between the input v_k and the contemporaneous received signal r_{k-n} as in Figure 2 for the successful (i.e. burst-free with small estimation error) functioning of the adaptive echo canceller. Wide-band signal inputs and substantial loop delay can provide such a decorrelation. Finally, a 'new' double-talk detector threshold test signal has been proposed which could lead to the development of guidelines for the improved design of adaptive echo cancellation systems.

ACKNOWLEDGEMENTS

The authors thank C. E. Rohrs of Tellabs Research Laboratory for introducing them to the issue of bursting in adaptive hybrid loops and J. B. Kenney of Tellabs Research Laboratory for answering their many questions about double-talk detector technology.

This work is supported in part by NSF Grant MIP-8608787.

APPENDIX

Proof of Proposition 1

Rewrite the updating algorithm of (1) as

$$\tilde{h}_k = \tilde{h}_{k-1} - \mu s_k r_{k-n} \tag{31}$$

Over a period of N samples the update becomes

$$\tilde{h}_{k+N} = \tilde{h}_k - \mu \sum_{i=1}^{N} s_{k+i} r_{k+i-n} \tag{32}$$

If μ is small enough, we can approximate

$$\tilde{h}_{k+i} \approx \tilde{h}_k, \quad i = 1, 2, \ldots, N-1 \tag{33}$$

If $|\alpha\tilde{h}_k| < 1$, (32) can be rewritten as

$$\alpha\tilde{h}_{k+N} = \alpha\tilde{h}_k - \mu N \Delta(\alpha\tilde{h}) \tag{34}$$

where from (15) and the approximation of (7), (8) we have

$$\begin{aligned}\Delta(\alpha\tilde{h}_k) &\triangleq \frac{\alpha}{N}\sum_{i=1}^{N} s_{k+i} r_{k+i-n} \approx \alpha \operatorname{Avg}\{s_{k+i} r_{k+i-n}\} \\ &= \frac{0{\cdot}5\alpha^2 A_1^2 \cos(2n\omega_1)}{1 + (\alpha\tilde{h}_k)^2 - 2\alpha\tilde{h}_k \cos(2n\omega_1)} + \frac{0{\cdot}5\alpha\tilde{h}_k A_2^2}{1 + (\alpha\tilde{h}_k)^2 - 2\alpha\tilde{h}_k \cos(2n\omega_2)}\end{aligned} \tag{35}$$

Notice that $\Delta(\alpha\tilde{h})$ is C^1 and $\Delta(\alpha\tilde{h}^*) = 0$. According to (17) we know that either $\alpha\tilde{h}^* \leqslant 0$ or $\alpha\tilde{h}^* \geqslant 0$. Suppose that $0 < \alpha\tilde{h}^* < 1$, then from (17) we have $\cos(2n\omega_1) < 0$. But then

$$\Delta(0) = 0{\cdot}5\alpha^2 A_1^2 \cos(2n\omega_1) < 0 \tag{36}$$

From the assumption, $\Delta(\alpha\tilde{h}) \neq 0$ for $\alpha\tilde{h} \in (-1, 0]$. Thus, owing to its continuity, $\Delta(\alpha\tilde{h})$ does not change sign in $(-1, 0]$ and hence from (36)

$$\Delta(\alpha\tilde{h}) < 0, \quad \forall \alpha\tilde{h} \in (-1, 0] \tag{37}$$

Also,

$$\frac{\partial}{\partial \alpha\tilde{h}} \Delta(\alpha\tilde{h}) = \frac{\alpha^2 A_1^2 [\cos^2(2n\omega_1) - \alpha\tilde{h} \cos(2n\omega_1)]}{[1 + (\alpha\tilde{h})^2 - 2(\alpha\tilde{h})\cos(2n\omega_1)]^2} + \frac{A_2^2 [1 - (\alpha\tilde{h})^2]/2}{[1 + (\alpha\tilde{h})^2 - 2(\alpha\tilde{h})\cos(2n\omega_2)]^2} \tag{38}$$

Since $\cos(2n\omega_1) < 0$, it is immediate that

$$\frac{\partial}{\partial \alpha\tilde{h}} \Delta(\alpha\tilde{h}) > 0, \quad \forall \alpha\tilde{h} \in [0, 1) \tag{39}$$

$\Delta(\alpha\tilde{h})$ is monotonic in $[0, 1)$. Therefore $\alpha\tilde{h}^*$ must be the unique zero-crossing point in $[0, 1)$ and is thus unique in $(-1, 1)$. Also, $\alpha\tilde{h}^*$ is locally stable according to (39). Furthermore, for $0 < \alpha\tilde{h}^* < 1$ we have

$$\begin{aligned}&\Delta(\alpha\tilde{h}) < 0, \quad \forall \alpha\tilde{h} \in (-1, \alpha\tilde{h}^*) \\ &\Delta(\alpha\tilde{h}) > 0, \quad \forall \alpha\tilde{h} \in (\alpha\tilde{h}^*, 1)\end{aligned} \tag{40}$$

Similarly, it can be shown for $-1 < \alpha\tilde{h}^* < 0$ that (40) holds. If $\alpha\tilde{h}^* = 0$, then $\cos(2n\omega_1) = 0$ and from

(38) we have

$$\frac{\partial}{\partial \alpha\tilde{h}}\Delta(\alpha\tilde{h}) = \frac{A_2^2[1-(\alpha\tilde{h})^2]/2}{[1+(\alpha\tilde{h})^2-2(\alpha\tilde{h})\cos(2n\omega_2)]^2} > 0, \quad \forall \alpha\tilde{h} \in (-1,1) \tag{41}$$

Hence $\alpha\tilde{h}^* = 0$ is locally stable, for which (40) also holds.

The result of (40) shows through (34) that for $|\alpha\tilde{h}^*| < 1$, if $-1 < \alpha\tilde{h}_k < \alpha h^*$, then over the period of N iterations $\alpha\tilde{h}_k$ will be approximately reduced by $\mu N \Delta(\alpha\tilde{h}_k)$, where $\Delta(\alpha\tilde{h}_k) < 0$, and if $\alpha\tilde{h}^* < \alpha\tilde{h} < 1$, then over N iterations $\alpha\tilde{h}_k$ will be approximately reduced by $\mu N \Delta(\alpha\tilde{h}_k)$, where $\Delta(\alpha\tilde{h}_k) > 0$. Thus, in either case, $\alpha\tilde{h}^*$ is locally stable, and if $|\alpha\tilde{h}_k| < 1$, $\alpha\tilde{h}_k$ will be moving towards the average equilibria $\alpha\tilde{h}^*$, eventually settling in the neighbourhood of $\alpha\tilde{h}^*$.

Proof of Proposition 2

Suppose that all the solutions to (16) have magnitudes $|\alpha\tilde{h}^*| > 1$. Consider the case $\cos(2n\omega_1) > 0$ for which (17) dictates that $\alpha\tilde{h}^* < -1$. Now assume bursting has not occurred and at the time instant k

$$\alpha\tilde{h}^* < -1 < \alpha\tilde{h}_k < 1 \tag{42}$$

Then using the results in the proof of Proposition 1 we have

$$\Delta(\alpha\tilde{h}) \neq 0, \quad \forall \alpha\tilde{h} \in (-1,1) \tag{43}$$

From the continuity of $\Delta(\alpha\tilde{h})$ and the fact that

$$\Delta(0) = 0{\cdot}5\alpha^2 A_1^2 \cos(2n\omega_1) > 0 \tag{44}$$

we can conclude that for $\alpha\tilde{h}^* < -1$

$$\Delta(\alpha\tilde{h}_k) > 0, \quad \forall \alpha\tilde{h} \in (-1,1) \tag{45}$$

This result indicates that if $\tilde{h}_k$ is such that $|\alpha\tilde{h}_k| < 1$, then over the period of N iterations $\alpha\tilde{h}_k$ is going to be reduced approximately by $\mu N \Delta(\tilde{h}_k)$, where $\Delta(\tilde{h}_k) > 0$. Thus $\alpha\tilde{h}_k$ will move towards the stability boundary $|\alpha\tilde{h}| = 1$. This motion will continue until $\Delta(\alpha\tilde{h}_k) \leqslant 0$. But since (45) is true, $\alpha\tilde{h}_k$ will continue moving towards the stability boundary until reaching or crossing it. Thus, assuming (42), $\alpha\tilde{h}_k$ will either move across the stability boundary and bursting thus occurs, or approach arbitrarily close to the stability boundary without crossing it.

The proof is similar for $\alpha\tilde{h}^* > 1 > \alpha\tilde{h}_k > -1$ when $\cos(2n\omega_1) < 0$.

Proof of Proposition 3

The proof is trivial if $\cos(2\omega_1) = 0$, so assume $\cos(2\omega_1) \neq 0$. Let $x = \alpha\tilde{h}^*$ and let

$$K = \frac{|1 - xe^{-j2n\omega_2}|^2}{|1 - xe^{-j2n\omega_1}|^2}\cos(2n\omega_1) = \frac{1 + x^2 - 2x\cos(2n\omega_2)}{1 + x^2 - 2x\cos(2n\omega_1)}\cos(2n\omega_1) \tag{46}$$

It then follows that

$$\frac{K(1+x^2)}{\cos(2n\omega_1)} - 2xK = 1 + x^2 - 2x\cos(2n\omega_2) \tag{47}$$

If $\cos(2n\omega_1) > 0$, then $x = \alpha\tilde{h}^* < 0$ from (17) and $K > 0$ from (46). Therefore

$$K(1+x^2) - 2xK \leqslant \frac{K(1+x^2)}{\cos(2n\omega_1)} - 2xK = 1 + x^2 - 2x\cos(2n\omega_2) \leqslant 1 + x^2 - 2x \tag{48}$$

Hence $K(1-x)^2 \leqslant (1-x)^2$ and consequently $K \leqslant 1$. If $\cos(2n\omega_1) < 0$, then $x > 0$ and $K < 0$. Therefore

$$-K(1+x^2) - 2x \leqslant \frac{K(1+x^2)}{\cos(2n\omega_1)} - 2xK = 1 + x^2 - 2x\cos(2n\omega_2) \leqslant 1 + x^2 + 2x \tag{49}$$

Thus $K \geqslant -1$. It can hence be concluded that

$$|K| = \left| \frac{|1 - \alpha\tilde{h}^* e^{-j2n\omega_2}|^2}{|1 - \alpha\tilde{h}^* e^{-j2n\omega_1}|^2}\cos(2n\omega_1) \right| \leqslant 1 \tag{50}$$

Proof of Proposition 4

If $\cos(2n\omega_1) = 0$, then $\alpha\tilde{h}^* = 0$ is the only equilibrium and bursting can be avoided no matter what M is. Thus (ω_1, ω_2) pairs exist such that some solutions of (18) satisfy $|\alpha\tilde{h}^*| < 1$.

On the other hand, if $\cos(2n\omega_1) \neq 0$, for any $M > 1$, i.e.

$$M = 1 + \varepsilon, \quad \varepsilon > 0 \tag{51}$$

we can find an ω_1 and ω_2 such that

$$\cos(2n\omega_2) = \frac{1 + 2\delta}{1 + \varepsilon} \quad \text{and} \quad \cos(2n\omega_1) = \frac{1 + \delta}{1 + \varepsilon + 2(1 + \delta)\delta/[1 + (1 + \delta)^2]} \tag{52}$$

where $0 < \delta < \varepsilon/2$, which results in $\alpha\tilde{h}^* = -(1 + \delta) < -1$ as solution to (18). Hence (ω_1, ω_2) pairs also exist such that some solutions satisfy $|\alpha\tilde{h}^*| > 1$ and bursting may occur.

REFERENCES

1. Sondhi, M. M. and A. J. Presti, 'A self-adaptive echo canceler', *Bell Syst. Tech. J.*, **45**, 1851–1854 (1966).
2. Weinstein, S. B., 'Echo cancellation in the telephone network', *IEEE Commun. Soc. Mag.* **15**, 9–15 (1977).
3. Sondhi, M. M. and D. A. Berkeley, 'Silencing echoes on the telephone network', *Proc. IEEE*, **68**, 948–963 (1980).
4. Duttweiler, D. L., 'A twelve-channel digital echo canceler', *IEEE Trans. Commun.*, **COM-26**, 647–653 (1978).
5. Sethares, W. A., C. R. Johnson Jr. and C. E. Rohrs, 'Bursting in adaptive hybrids', *IEEE Trans. Commun.*, **COM-37**, 791–799 (1989).
6. Anderson, B. D. O., 'Adaptive systems, lack of persistency of excitation and bursting phenomena', *Automatica*, **21**, 247–258 (1985).
7. Macchi, O. and M. Jaidane-Saidane, 'Quasi-periodic self-stabilization of adaptive ARMA predictors', *Int. j. adaptive control and signal processing*, **2**, 1–31 (1988).
8. Johnson, C. R., Jr., *Lectures on Adaptive Parameter Estimation*, Prentice-Hall, Englewood Cliffs, NJ, 1988, pp. 8–21, 126–134.